

FAST TRACK COMMUNICATION

Structural transitions of non-helical Au nanotubes induced by axial compression

Xiao Gu and Xin-Gao Gong

Surface Physics Laboratory, Department of Physics, Fudan University, Shanghai 200433, People's Republic of China

E-mail: xggong@fudan.edu.cn

Received 13 March 2007, in final form 10 April 2007

Published 25 May 2007

Online at stacks.iop.org/JPhysCM/19/242205

Abstract

Based on density functional calculations, we have found that axial compression can induce structural transitions between $\text{Au}(n, n)$ and $\text{Au}(2n, n)$ nanotubes. The corresponding energy barriers increase with n . Although $\text{Au}(2n, n)$ nanotubes are energetically more stable, the energy difference between $\text{Au}(n, n)$ and $\text{Au}(2n, n)$ decreases with n . The structural transitions are believed to be unique in those nanotubes with metallic bonds, while nanotubes with covalent bonds, such as carbon nanotubes, will not have these features.

(Some figures in this article are in colour only in the electronic version)

1. Introduction

Studies of low-dimensional nano systems such as carbon nanotubes (CNT), Si nanowires [1] and boron nitride nanotubes [2, 3] are becoming popular. Recently, Au nanowires and nanotubes have attracted much attention [4–11]. Direct experimental transmission electron microscopy (TEM) observations have unveiled Au nanotubes (AuNT) among Au nanowires [12]. More recently, helical $\text{Au}(5, 3)$ nanotubes have been synthesized at 150 K by irradiating a thin Au film with an electron beam [13], and corresponding numerical simulations showed the result to be in satisfactory agreement with the TEM images of $\text{Au}(5, 3)$ [14]. Although non-helical single-wall Au nanotubes have not been observed through the experiments, geometrical structures and electronic properties of these nanotubes, both helical and non-helical, have been discussed theoretically using the density functional theory (DFT) method [14–16]. In this letter, we report unique structural transitions in single-wall Au nanotubes. When compression is applied along the axis of the nanotube, structural transitions can be induced to release the increased stress.

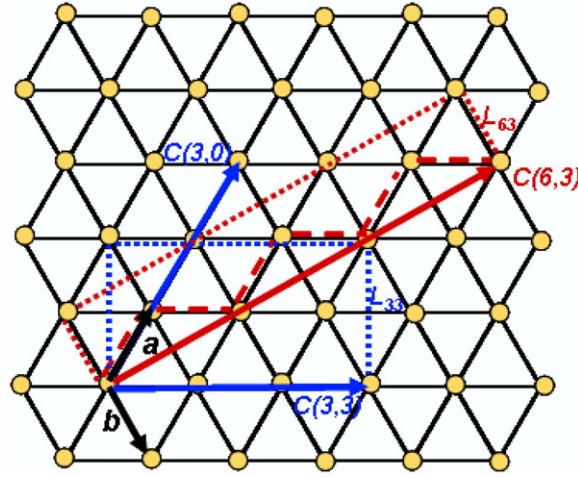


Figure 1. A sheet of gold atoms. Similar to a carbon nanotube, an Au nanotube could be formed by folding the sheet. The basis vectors \vec{a} and \vec{b} are used to identify the Au nanotube, and the vector $\vec{C}(m, n)$ represents such identifications. $\vec{C}(m, n)$ is defined as $m\vec{a} + n\vec{b}$. The vectors of $\vec{C}(3, 3)$, $\vec{C}(3, 0)$ and $\vec{C}(6, 3)$ are shown in particular, consequently $\vec{C}(3, 3)$ and $\vec{C}(3, 0)$ are equivalent. The dotted lines sketch out one super-cell of the AuNTs; L_{33} and L_{63} are the axial lengths of Au(3, 3) and Au(6, 3), respectively. The number of atoms in the unit cell is $2n$ in both Au(n, n) and Au($2n, n$).

2. Computational details

Based on the density functional theory with general gradient approximation (GGA) [17], we have carried out calculations on Au nanotubes with the VASP code [18]. The wavefunctions are expanded in plane waves. A super cell with edge length $25 \text{ \AA} \times 25 \text{ \AA} \times L$ is used with periodic boundary condition (PBC), where L is the length of the AuNT in the super cell, and Monkhorst grid of $1 \times 1 \times 10$ is used for k -point sampling in Brillouin zone. Only the valence electrons are treated explicitly and their interaction with ionic cores are described by the projector augmented-wave (PAW) pseudo-potentials [19, 20]. The scalar relativistic effects are included in the calculations, which is very important in Au nano-systems [21–23].

Au nanotubes could be regarded as rolling up a gold sheet of specified finite width and certain length. As shown in figure 1, all the gold atoms are located at the lattice sites of a two-dimensional (2D) triangular lattice, instead of hexagonal lattice of a carbon sheet. The basis lattice vectors \vec{a} and \vec{b} are used to define the 2D lattice. A vector $\vec{C}(m, n)$ is defined as $\vec{C} = m\vec{a} + n\vec{b}$, where m, n are integers. With \vec{C} , we can specify any Au nanotube as Au(m, n) [11]. The vector $\vec{C}(m, n)$ of the Au sheet generates a nanotube of Au(m, n) with length L along the axial direction. This principle is directly extended from that of carbon nanotubes, however the difference between two systems is obvious. For AuNT, the 2D unit cell has only one atom while it has two for carbon sheet. Consequently, the vector $\vec{C}(n, n)$ is equivalent to $\vec{C}(n, 0)$. For instance, in figure 1, $\vec{C}(3, 3)$ and $\vec{C}(3, 0)$ are equivalent to each other and lead to the same nanotube, Au(3, 3).

Accordingly, the nanotubes Au(m, n) can simply be divided into two types: helical and non-helical [11]. When $m = n$ or $m = 2n$, the nanotube is non-helical, such as Au(5, 5). When $m \neq n$ and $m \neq 2n$, the nanotube is helical, such as Au(5, 3). In the present letter, we pay attention only to the non-helical systems. The AuNTs, based on $\vec{C}(3, 3)$ and $\vec{C}(6, 3)$ shown in figure 1, are two typical non-helical AuNTs. It is noticeable that each of the Au(n, n)

Table 1. Properties of non-helical Au nanotubes. R_d : diameters of the nanotubes, L : length (axial direction), R_b : average bond length, E_d : the total energy per atom, G : $\partial^2 E / \partial \epsilon^2$ (where ϵ is the axial strain).

AuNTs	R_d (Å)	L (Å)	R_b (Å)	E_d (eV)	G (eV)
(3, 3)	1.73	4.30	2.88	−2.44	37.9
(6, 3)	2.44	2.75	2.80	−2.71	79.0
(5, 5)	2.46	4.60	2.82	−2.68	92.3
(10, 5)	3.90	2.75	2.77	−2.84	174.4
(6, 6)	2.80	4.70	2.78	−2.76	168.3
(12, 6)	4.66	2.75	2.77	−2.87	213.9
(8, 8)	3.66	4.70	2.78	−2.82	256.7
(16, 8)	6.15	2.75	2.78	−2.90	288.4

and $\text{Au}(2n, n)$ has the same $2n$ atoms in the unit cell and that the energy difference between $\text{Au}(n, n)$ and $\text{Au}(2n, n)$ decreases with n increasing, as shown in table 1.

3. Results and discussion

Our calculations have revealed that $\text{Au}(n, n)$ nanotubes should transit to $\text{Au}(2n, n)$ nanotubes under axial compression. Figure 2 shows a schematic of the structural changes from $\text{Au}(n, n)$ to $\text{Au}(2n, n)$. When the applied compression on $\text{Au}(n, n)$ increases, the radius of the nanotube increases, as shown in figure 2(a). Meanwhile, as shown in figure 2(b), the vertical bond is broken by the strain, while the other two horizontally positioned atoms are forced to move closer, and finally bond together to complete a structural transition. Detailed analysis shows that the new structure is the $\text{Au}(2n, n)$ nanotube, as shown in the right-hand column of figure 2(a). This means that a transition driven by the axial compression from $\text{Au}(n, n)$ to $\text{Au}(2n, n)$ occurs.

The smaller the n , the larger the energy difference between $\text{Au}(n, n)$ and $\text{Au}(2n, n)$ and the smaller the energy barrier from $\text{Au}(n, n)$ to $\text{Au}(2n, n)$, as shown in figure 3. In this transition process, as table 1 shows, the radius of the AuNT increases more quickly with n , compared to the variation in the length L . The radius of $\text{Au}(3, 3)$ is 1.73 Å, and the value increases to 2.44 Å in $\text{Au}(6, 3)$. Meanwhile, it can be seen in figure 3 that the transition energy barrier for $\text{Au}(3, 3)$ to $\text{Au}(6, 3)$ is only about 0.03 eV/atom, indicating that it should be very easy for the transition to occur. However, the total energy of the $\text{Au}(6, 3)$ is −2.71 eV/atom, which is much lower than that of the $\text{Au}(3, 3)$, −2.44 eV. Thus it should be much more difficult for the reverse process to occur. Actually, the backward barrier is about 0.30 eV/atom. This means that the $\text{Au}(3, 3)$ might not be stable against compression; the transition from $\text{Au}(3, 3)$ to $\text{Au}(6, 3)$ would be favourable. We have also found that the $\text{Au}(5, 5)$, $\text{Au}(6, 6)$ and $\text{Au}(8, 8)$ could have similar transitions. In the case of $\text{Au}(5, 5)$ to $\text{Au}(10, 5)$, the increment in the radius is about 1.44 Å, compared to 0.71 Å for the case of $\text{Au}(3, 3)$ to $\text{Au}(6, 3)$, listed in table 1. The total energy difference between $\text{Au}(5, 5)$ and $\text{Au}(10, 5)$ is only 0.16 eV/atom, while the transition barrier increases to about 0.11 eV/atom, and that for the reverse transition is about 0.28 eV/atom. The energy barriers of the transition between $\text{Au}(n, n)$ and $\text{Au}(2n, n)$ increases with n , as shown in figure 3. Since the volumes of the nanotubes are not well defined [24], we have calculated the second derivative of the total energy to the axial strains: $G = \partial^2 E / \partial \epsilon^2$, where ϵ is the axial strain. As listed in table 1, the value of G increases with n , and the values of G for $\text{Au}(n, n)$ are smaller than those for $\text{Au}(2n, n)$.

We have shown $\text{Au}(n, n)$ nanotubes can experience the transition to $\text{Au}(2n, n)$ when $n = 3, 5, 6, 8$. What will happen for $n = 4, 7$? Interestingly, an intermediate structure, which

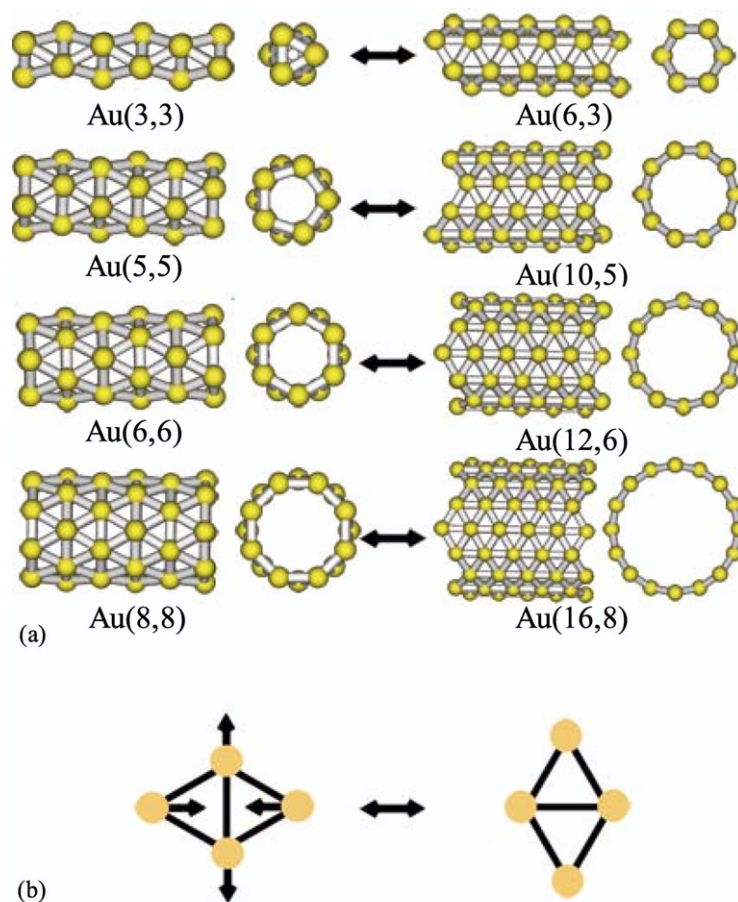


Figure 2. (a) Transitions under axial compression of non-helical AuNTs. The left columns show the Au(3, 3), Au(5, 5), Au(6, 6) and Au(8, 8) NTs, and the right columns show Au(6, 3), Au(10, 5), Au(12, 6) and Au(16, 8) respectively. The details of the geometrical properties are listed in the table 1. (b) The bond changes during the transition from Au(n, n) to Au($2n, n$). The left one stands for the Au(n, n) and the arrows indicate the movement of the atoms during the axial compression increasing. The final state of the Au($2n, n$) is shown on the right.

is double-wall-like (DW-like) AuNT, is found during the transition. In Au(4, 4), there are two four-atom rings with a relative orientation of 90° , as shown in figure 4(a). When axial compression is applied, only one four-atom ring (A–B–C–D) is broken, while the other (E–F–G–H) survives. The four atoms of the broken ring are re-located on a ring with a larger radius. Actually, the radius of this DW-like nanotube is about 7.00 Å compared to 3.95 Å of the Au(4, 4). During this process, the radius of the inner ring (E–F–G–H) actually increases as well, although only slightly, from 3.95 to 4.13 Å. As to the transition towards Au(8, 4), both of two four-atom rings are required to break, simultaneously, and then they can connect together to form a new complete ring with an even larger radius. We have noticed that Au(8, 4) is more stable than the DW-like AuNT by about 0.12 eV/atom. As mentioned above, the SW Au(4, 4) has two four-atom rings, but during the transition only one of them is broken, while in the case of the transition of Au(n, n) to Au($2n, n$), where $n = 3, 5, 6, 8$, both of the rings are broken. Therefore, the only requirement for Au(8, 4) is to break the survival ring (E–F–G–H) with a

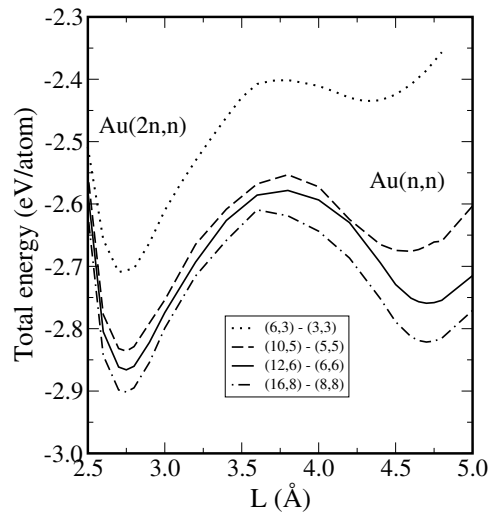


Figure 3. The total energy of AuNTs as a function of unit cell length. The minima around 4.3–4.7 Å are for $Au(n, n)$, while the minima around 2.7 Å are for $Au(2n, n)$. The barrier from $Au(n, n)$ to $Au(2n, n)$ increases with increasing n .

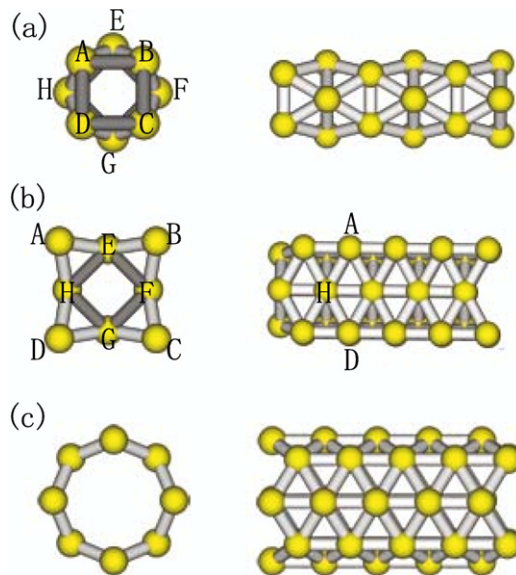


Figure 4. Transition from $Au(4, 4)$ to intermediate DW-like NT then to $Au(8, 4)$. The top panel (a) is for $Au(4, 4)$, (b) is the intermediate structure, and (c) is the $Au(8, 4)$. Two four-atom rings (A–B–C–D and E–F–G–H) can be seen.

small energy barrier, about 0.01 eV/atom. Such a small barrier leads us to believe that the final state of the $Au(4, 4)$ transition will also be $Au(8, 4)$. The present calculation shows that $Au(7, 7)$ has similar behaviour.

In figure 5, we show the band structures of some selected Au nanotubes. As expected, all the Au nanotubes are metallic. It clearly shows similar bands in $Au(n, n)$ nanotubes, and also in

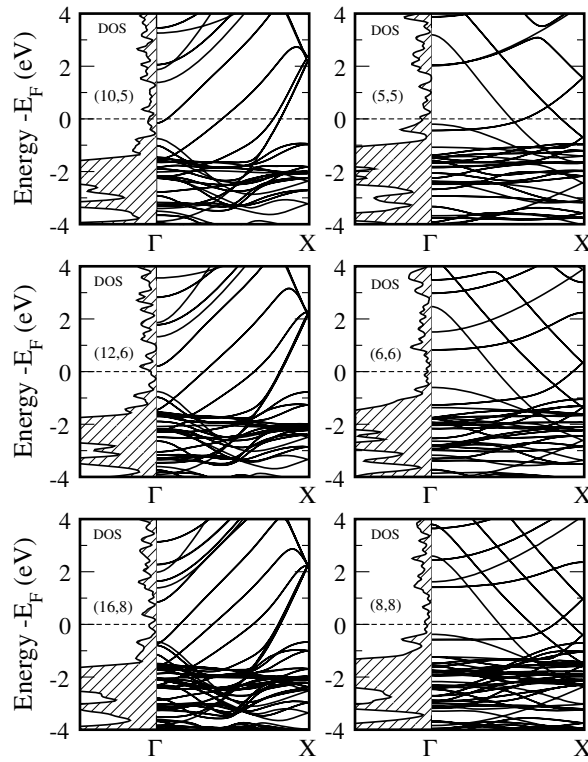


Figure 5. The band structures of $Au(n, n)$ and $Au(2n, n)$, where $n = 5, 6, 8$. The right ones are for the $Au(n, n)$ and the left ones are for the $Au(2n, n)$. The Fermi energies are shifted to zero.

$Au(2n, n)$, however they are different between $Au(n, n)$ and $Au(2n, n)$. Compared to $Au(n, n)$, the band widths of $Au(2n, n)$ have increased by about 0.5 eV, which is mainly due to the shift of s bands to higher energy. As listed in table 1, the bond lengths of $Au(2n, n)$ are shorter than those of $Au(n, n)$, which leads to the delocalization of the s electrons, resulting in a reduction of the interaction of s and d electrons.

The properties of AuNTs discussed above, which were not observed in CNTs, can be attributed to the metallic bond. The bond length of Au–Au bond is about 2.8 Å and the binding energy is about 2.6–2.9 eV/atom, which is much easier to break, while the bond length between carbon atoms is only about 1.4 Å with much higher binding energy. It is possible to break the constrained Au bond to lower the energy and release the strains.

4. Conclusion

In summary, we have studied the structural properties of Au nanotubes, which are remarkably different from those of CNTs. $Au(n, n)$ can be transferred to $Au(2n, n)$ under an axial compression. $Au(n, n)$ follows directly the transition path towards $Au(2n, n)$, for $n = 3, 5, 6, 8$, while when $n = 4, 7$ there would be intermediate structures towards $Au(2n, n)$. All these unique properties could probably originate from the soft Au–Au bonds.

Acknowledgments

The present work is partially supported by the National Science Foundation of China, the special funds for the Major State Basic Research and Research Program of Shanghai. The

main computation was performed on the teracluster LSSC-II in the State Key Laboratory of Scientific and Engineering Computing (LSEC), and also in the Supercomputer Center of Fudan University, the Supercomputer Center of Shanghai.

References

- [1] Ma D D D, Lee C S, Au F C K, Tong S Y and Lee S T 2003 *Science* **299** 1874
- [2] Chopra N G, Luyken R J, Cherrey K, Crespi V H, Cohen M L, Louie S G and Zettl A 1995 *Science* **269** 966
- [3] Vaccarini L, Goze C, Henrard L, Hernandez E, Bernier P and Rubio A 2000 *Carbon* **38** 1681
- [4] Ohnishi H, Kondo Y and Takayanagi K 1998 *Nature* **395** 780
- [5] Mokrousov Y, Bihlmayer G and Blugel S 2005 *Phys. Rev. B* **72** 045402
- [6] Yang B, Kamiya S, Yoshida K and Shimizu T 2004 *Chem. Comm.* 500
- [7] Wirtz M and Martin C R 2003 *Adv. Mater.* **15** 455
- [8] Wang H W, Shieh C F, Chen H Y, Shiu W C, Russo B and Cao G Z 2006 *Nanotechnology* **17** 2689
- [9] Lin J S, Ju S P and Lee W J 2005 *Phys. Rev. B* **72** 085448
- [10] del Valle M, Tejedor C and Cuniberti G 2006 *Phys. Rev. B* **74** 045408
- [11] Tosatti E, Prestipino S, Kostmeier S, Dal Corso A and Di Tolla F D 2001 *Science* **291** 288
- [12] Kondo Y and Takayanagi K 2000 *Science* **289** 606
- [13] Oshima Y and Onga A 2003 *Phys. Rev. Lett.* **91** 205503
- [14] Yang X P and Dong J M 2005 *Phys. Rev. B* **71** 233403
- [15] Yang C K 2004 *Appl. Phys. Lett.* **85** 2923
- [16] Senger R T, Dag S and Ciraci S 2004 *Phys. Rev. Lett.* **93** 196807
- [17] Perdew J P and Wang Y 1992 *Phys. Rev. B* **45** 13244
- [18] Moroni E G, Kresse G, Hafner J and Furthmuller J 1997 *Phys. Rev. B* **56** 15629
- [19] Blöchl P E 1994 *Phys. Rev. B* **50** 17953
- [20] Kresse G and Joubert D 1999 *Phys. Rev. B* **59** 1758
- [21] Li J, Li X, Zhai J H and Wang L S 2003 *Science* **299** 864
- [22] Gu X, Ji M, Wei S H and Gong X G 2004 *Phys. Rev. B* **70** 205401
- [23] Ji M, Gu X, Li X, Gong X G, Li J and Wang L S 2005 *Angew. Chem. Int. Edn* **44** 7119
- [24] Hernandez E, Goze C, Bernier P and Rubio A 1998 *Phys. Rev. Lett.* **80** 4502